ISSN 2179-3956

DRY SLIDING WEAR BEHAVIOR OF HARD CHROMIUM AND NICKEL-BASED COATINGS IN BALL ON RING TEST[1]

Marcelo J.L. Gines[2]
Walter Tuckart[3]
Sebastián Abraham[3]

Abstract
This study addresses the dry sliding wear behavior of different hard chromium coatings and they are compared to mono and multilayered nickel-based coatings which could be a replacement of conventional hard chromium coatings. Both hard chromium and nickel-based coatings were obtained over a substrate of AISI H13 steel by electroplating from hexavalent chromium and nickel-tungsten-phosphorus aqueous solutions, respectively. Monolayer hard chromium coatings were prepared by changing current density, temperature, and bath composition (proprietary non-fluoride catalyst). Mono and multilayered nickel-based coatings were prepared by using various current densities leading to different structure and composition, and consequently distinct mechanical properties. Scanning electron microscopy and X-ray diffraction were employed to assess the morphology and microstructure of the coatings. According the wear test results, nickel-based coatings were less prone to wear than hard chromium coatings even though the latter are harder (hard chromium: 900-1100 HV; nickel-based: 500-600 HV). This behavior might be attributable to different wear mechanisms: abrasive wear type plowing for nickel-based coatings and adhesive wear for hard chromium coatings.
Key words: Hard chromium; Nickel-based coatings; Wear sliding; Nanoestructered coatings.

[1] *Technical contribution to the First International Brazilian Conference on Tribology – TriboBr-2010, November, 24th-26th, 2010, Rio de Janeiro, RJ, Brazil.*
[2] *Surface and Coating Department, REDE-AR, TenarisSiderca, Dr. Simini 250, 2804 Campana, Buenos Aires, Argentina.*
[3] *Engineering Department, Universidad Nacional del Sur, Av. Alem 1253, 8000, Bahía Blanca, Buenos Aires, Argentina.*

ISSN 2179-3956

1 INTRODUCTION

Chromium coatings prepared from hexavalent chromium (Cr^{6+}) electroplating bath are widely employed for improving hardness, wearability, erosion resistance and decorative appearance of engineering tools and several components,[1-4] even though the high-power consumption and the huge evolution of hydrogen in the process. However, the use of hexavalent Cr presents potentially serious health and environmental problems.[5] Moreover, there has been a considerable effort to find adequate replacements of Cr and Cr-based coatings to eliminate the use of hexavalent Cr. Potential process substitutions for hard chromium plating include electroless nickel, several nickel-tungsten options, and spray applications such as plasma spray or high-velocitiy oxygen fuel (HVOF) coatings. Among electroplating options, cobalt-based and nickel-based electroplated coatings has been proposed as potential alternatives[6,7] as well as multilayered coatings which possess a number of very interesting enhanced or novel properties.[8]

We have studied the physicochemical and mechanical properties of Ni-W-P coatings onto steel by pulsed current as a function of phosphorus content and annealing temperature as potential replacement of hard chromium to be used at high temperature,[9] but the tribological behavior was unexplored. We found that adding small quantities of P increases the microhardness temperature resistance of nanoestructured Ni-W coatings significantly. Furthermore, improved Ni-W-P coatings have better microhardness temperature resistance than hard chromium coatings.

On the other hand, Ni-P coatings were proposed as hard chromium replacements but their wear resistance properties were not high enough.[10] However, combining the Ni-P properties and the multilayered coatings approach, the wear resistance might be improved.

In this work, the dry sliding wear behavior at room temperature of different hard chromium coatings is analized and they are compared to mono and multilayered nickel-based coatings which could be a replacement of conventional hard chromium coatings.

2 MATERIALS AND METHODS

2.1 Coating Preparation

All coatings were electrodeposited on cylinders of hardened and quenched AISI H13 steel mechanically polished to 600 grids.

The hard chromium (HC) electroplated samples were prepared in a custom heated glass cell and the anode was made of a lead-based alloy. The electrolytic bath employed is based on hexavalent chromium, with a composition reported in the literature as Sargent bath or conventional bath: chromic and sulfuric acid. [1-4] Additionally, a commercial 20% v/v non-fluoride catalyst-containing plating bath was prepared in the same way that the conventional ones. Prior to electrodeplating, AISI H13 steel substrate was thoroughly degreased with acetone and submitted to an anodic etching treatment in the plating solution employing an anodic charge of 1500 C/dm^2. All plating experiments were done at 20 A/dm^2 by using direct current (DC), and the cathode was rotated at 2 rpm.

Electroplating of Ni-W and Ni-W-P was performed in a jacketed glass cell containing the electroplating bath, which was agitated by rotating the cathode at 500 rpm. All

ISSN 2179-3956

experiments were conducted at a constant temperature of 75°C and the pH was kept at 9.0-9.5. Platinum mesh as well as DSA was employed as anodes and both direct (DC) and pulsed or alternate current (AC) was employed. Before electrodeplating, AISI H13 steel substrate was thoroughly degreased with acetone and submitted to an anodic/cathodic pretreatment using a Ni Woods electroplating baths (nickel chloride and hydrochloric acid). Chemical composition of the Ni-W electrolytic plating bath consisted of nickel sulfate, nickel tungstate, sodium citrate, ammonium chloride as described elsewhere.[11,12] In order to carry out the co-deposition of P, different amounts sodium hypophosphite was added to the Ni-W electrolytic plating bath.[9]
Mono and multilayered Ni-P coatings were prepared by electrodepositon in a jacketed glass cell containing the electroplating bath, which was agitated by rotating the cathode at 6 rpm. All experiments were conducted at a constant temperature of 70°C and at pH of 3.1. Ni bulk was the anode and direct current (DC) was supplied. Prior to electrodeplating, AISI H13 steel substrate was thoroughly degreased with acetone and submitted to an anodic/cathodic pretreatment using a Ni Woods electroplating baths. The electroplating bath was made with nickel sulfate, nickel chloride, boric acid, and phosphorus acid.[13]
In all electroplating experiments current was supplied by a Dynatronix DPR 20-10-30 power supply.

2.2 Characterization Techniques

The surface morphology and polished cross sections of the as-deposited coatings and the tribosurface resulting from sliding wear tests were characterized by scanning electron microscopy (SEM) using XL 30 Philips equipment. Semi-quantitative chemical composition was determined by calibrated energy dispersive x-ray spectroscopy (EDS) in the SEM. The thicknesses of the coatings were measured by SEM, and were employed to determine the efficiency of the process. The phases were determined by X-rays diffraction (XRD) with an equipment Phillips X'Pert diffractometer with a CuK_{α}=1.5405 Á. From XRD data, the average Cr and Ni crystallite size was determined by measuring the line-broadening of the Cr (222) and Ni (111) peaks, after correcting for instrumental line-broadening using the Cauchy-Gaussian relationship.[14,15] Micro-hardness tests were conducted on metallurgically-prepared cross-sections of the electrodeposits, using a LECO micro-indenter model LM 247AT with a Vickers indenter (load range: 10-50 g). Ten measurements were made for each load and the ratio between the mean indentation diagonal and coating thickness was close to 5, ensuring that the measurement reflects the property of the coating, without convolution with the substrate or surface properties.

2.3 Sliding Wear Test

Dry sliding wear tests were carried out by employing a home made ball on ring system. The coated samples rotated at constant speed of 576 rpm (0.3 m/s) against 5 mm diameter WC ball used as the counter-body. The contact load was 10 N of normal load during a sliding distance total of 360 m. All the sliding wear experiments were run in a standard laboratory environment: 24 ± 1°C and 50-55% humidity relative. Wear quantification was achieve by measuring the thickness outside and in the center of wear

ISSN 2179-3956

track from cross-sectional SEM micrographs. Coating volume loss was calculated assuming that the counter-body remains unchanged. The reported results are an average of at least two tests. The friction coefficient (COF) was recorded during the test and the value was defined according to standard ASTM G 115- 04. The surface and cross-section of the worn samples were examined by SEM.

3 RESULTS AND DISCUSSION

3.1 Physicochemical and Mechanical Characterization

The current density as well as the plating temperature are the most critical parameters of HC electroplating process.[4,16] Additionally, it is known that the addition of a non-fluoride catalysts to the Sargent bath changes the properties of the coating.[17] The effects of bath temperature and the use of a commercial catalyst on the properties of the HC coating were explored. It was observed at naked eyes that as bath temperature decreases below 50°C samples were less bright. This observation can be attributed to different coating roughness, given that as roughness increases brightness decreases. The addition of the catalyst produces smoother and brighter surfaces without nodule formation (Figure 1). Some microcracks were observed on the surface of as-deposited coatings. These cracks are related to the evolution of hydrogen on the cathode, which is the most prevalent reaction during the chromium plating process. Hydrogen is incorporated into the deposit forming chromium hydrides that are partially decomposed to metallic chromium and hydrogen gas. Owing to this, the resulting volume change and produces cracking.

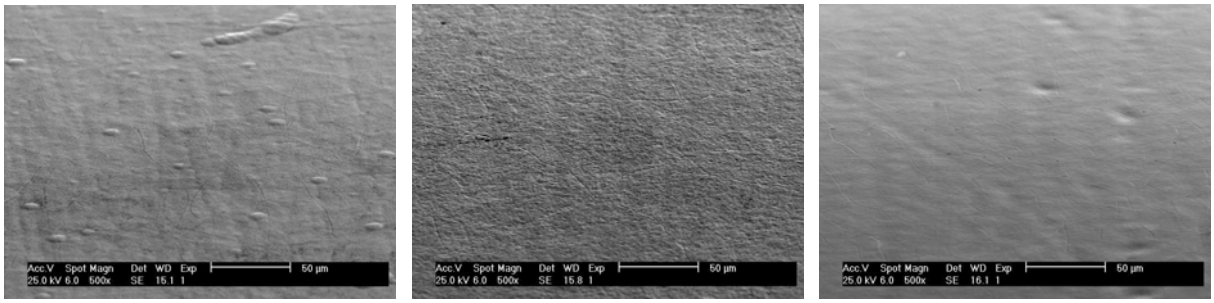

(a) (b) (c)

Figure 1. Top-down SEM micrograph of the HC samples (a) 20 A/dm^2, 50°C; (b) 20 A/dm^2, 60°C; (c) 20 A/dm^2, 50°C, non-fluoride additive.

In the cross-section the microcracks show a preferential orientation perpendicular to the substrate (Figure 2). They are distributed throughout their depth, could not be related to any special feature of the substrate, and none of them communicate the surface with the substrate. Clearly, it is observed that crack density diminishes when the temperature increases. It is worth mention that microcracks density and distribution strongly depends on bath chemistry. Conventional bath leads to the formation of coatings with low microcracks density (4000 cracks/mm^2, 15 μm), while non-fluoride catalyst-containing bath produces coatings with high microcracks density (14000 cracks/mm^2, 7 μm). This observation is important from two points of view: corrosion and wear resistance.[17,18] It was reported that sliding wear resistance increases as microcracks density increases.[19]

ISSN 2179-3956

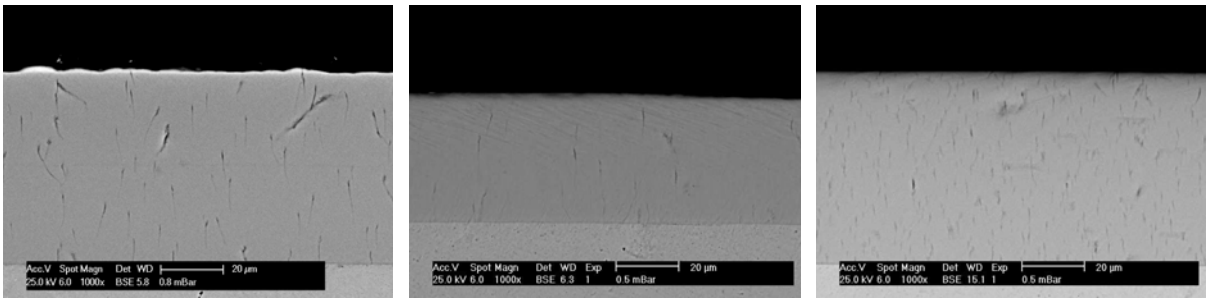

(a) (b) (c)

Figure 2. Cross-sectional SEM micrograph of the HC samples (a) 20 A/dm^2, 50°C; (b) 20 A/dm^2, 60°C; (c) 20 A/dm^2, 50°C, non-fluoride additive.

Also, it is worth noting that the coating thicknesses were different for each sample, even though the amount of transferred charge was the same. This observation is explained by the changes produced in the kinetics of the different cathodic reactions leading to a decrease of the efficiency as temperature rises and to a increase of the efficiency when the non-fluoride catalysts is added. Another feature is that HC coatings followed perfectly the substrate profile and there were no gaps or voids between the substrate and the coating, suggesting that the chromium adhesion to steel seems to be very good. XRD spectra from as-deposited HC coating as well as the grain sizes are shown in Figure 3. No major changes in the structure were observed for each bath. The most intense peaks are 211 (2θ=81.717°) and 222 (2θ=135.405°), even though other less intense peaks showed up. X-ray pattern of chromium are similar to that of iron, because both metals have a body centered cubic (BCC) structure and similar crystallographic parameter. Average crystallite size was calculated from 222 reflection and ranged from 5 to 10 nm, suggesting strongly that HC coating obtained by DC are nanocrystalline (Table 1). This result must be confirmed by TEM (Transmission Electron Microscopy). Microhardness values are shown in Table 1 and they ranged from 750 to 1150 kgf/mm^2, and are close to the expected hardness of HC coatings for this type of chemical bath.[4]

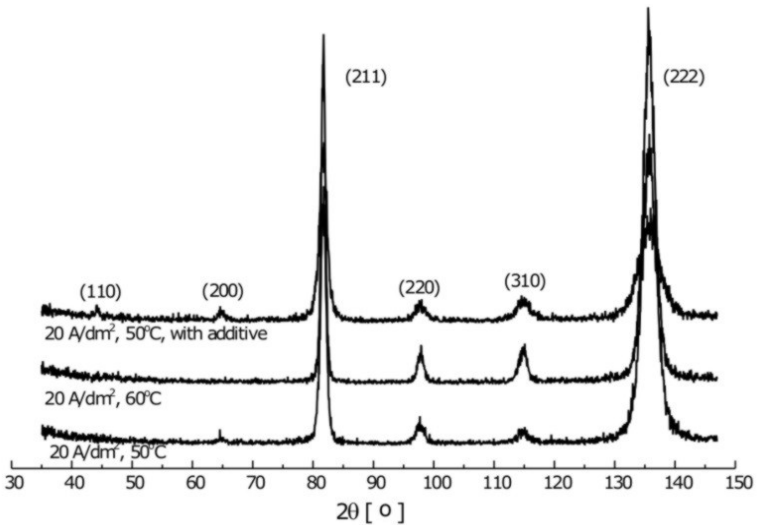

Figure 3. XRD patterns of HC samples.

ISSN 2179-3956

Table 1. Crystallite size and microhardness of HC coatings

Coating	Crystallite size [nm]	Microhardness [kgf/mm^2]
HC 20 A/dm^2, 50°C, conventional	8	960 ± 50
HC 20 A/dm2, 60°C, conventional	10	724 ± 34
HC 20 A/dm^2, 50°C, non-fluoride catalyst	5	1100 ± 31

The bath temperature had a strong effect on microhardness, the higher the bath temperature, the softer the coating. This observation might be due to chromium crystal size. According to the Hall-Petch relationship, hardness increases as crystal size diminshes: $H = H_0 + k\ D^{-n}$; where H is the hardness, H_0 is the hardness of very large grained material, k is a material constant, n is an exponent most often found to be equal to 0.5, and D the average grain size.[20] Similarly, HC coatings produced from non-fluoride catalyst-containing bath were harder than those from conventional bath.
Several Ni-P coatings were prepared as a function of current density in order to obtain coatings with different amount of phosphorus by using a single plating bath.
Table 2 shows the electroplating rate, the phosphorus content, the crystallite size obtained from XRD pattern, and the microhardness. The degree of phosphorus incorporation in the coating could be varied by simply changing the current density; as current density increases phosphorus content decreases. This feature allowed preparing multilayer Ni-P coatings using the same electroplating bath.

Table 2. Monolayer Ni-P coatings: electroplating rate, phosphorus content, crystallite size and microhardness

Current density [A/dm^2]	Plating rate [μm/min]	P content [wt.%]	Crystallite size [nm]	Microhardness [kgf/mm^2]
5	~ 30	14.4	1	528 ± 10
10	~ 75	12.2	4	540 ± 14
15	~ 135	9.1	4	596 ± 5
20	~ 195	6.4	5	646 ± 11
30	~ 290	5.0	7	653 ± 9

The incorporation of phosphorus changes their structure and mechanical properties. When the amount of phosphorus is low, the structure is crystalline where as when is high it is fully amorphous (Figure 4). The thickness of the coating was homogeneous across the substrate and generally ranged from 40 to 50 μm depending on the current density. All the coatings were compact and no cracks were observed.

ISSN 2179-3956

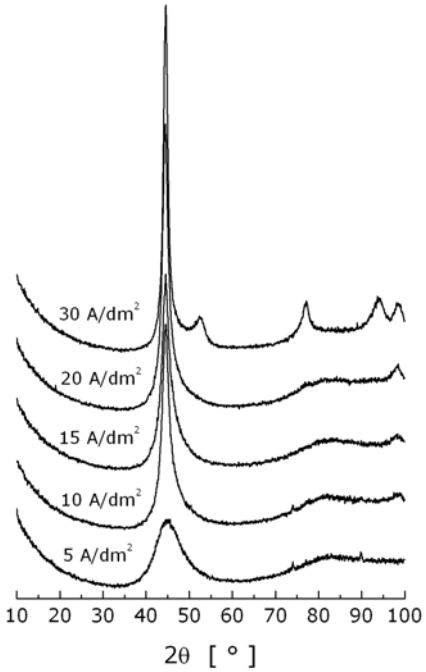

Figure 4. XRD patterns of Ni-P samples as a function of current density.

Some adhesion problems were observed for high current densities (higher than 15 A/dm^2) likely due to high internal stresses. Because of this, we decided to prepare multilayered Ni-P coatings (10, 50, 100, 1000 layers) alternating layer electroplated at 5 and 15 A/dm^2 in order to explore the multilayer effect on the wear resistance at room temperature as a function of the number of layers.
A detailed characterization of the morphology and structure of the Ni-W and Ni-W-P prepared using pulsed current can be found elsewhere.[9] Some morphological differences were observed when the coatings were obtained by using either AC or DC. The last led to less bright, more cracked and pitted coatings. A summary of the main properties of all the coatings are listed in Table 3.

Table 3. Chemical composition, crystallite size and microhardness of Ni-W and Ni-W-P coatings

Type	W content [wt.%]	P content [wt.%]	Crystallite size [nm]	Microhardness [kgf/mm2]
Ni-W AC	58.2	-	5	677 ± 12
Ni-W DC	61.2	-	3	673 ± 18
Ni-W-P AC	31.1	14.4	2	695 ± 11
Ni-W-P DC	28.2	9.4	2	589 ± 12

3.2 Sliding Wear Test

Table 4 lists the friction coefficient and the wear rate results obtained by each type of coating.

ISSN 2179-3956

Table 4. Friction coefficient and wear rate of HC, Ni-W and Ni-W-P coatings

Coating	COF	Wear Rate x 10^3 [mm^3/s]	Microhardness [kg/mm^2]
HC 20 A/dm^2, 50°C, conventional	0.69	0.357	960 ± 50
HC 20 A/dm2, 60°C, conventional	0.67	1.057	724 ± 34
HC 20 A/dm^2, 50°C, non-fluoride catalyst	0.69	0.248	1100 ± 31
Ni-W AC	0.48	0.003	677 ± 12
Ni-W DC	0.50	0.000	673 ± 18
Ni-W-P AC	0.53	0.005	695 ± 11
Ni-W-P DC	0.51	0.011	589 ± 12
Ni-P monolayer (5 A/dm^2)	0.61	1.696	528 ± 10
Ni-P monolayer (15 A/dm^2)	0.56	0.698	596 ± 5
Ni-P 10 layers	0.59	0.017	528 / 596
Ni-P 50 layers	0.35	0.007	528 / 596
Ni-P 100 layers	0.52	0.189	528 / 596
Ni-P 1000 layers	0.52	0.110	528 / 596

Regarding the wear rate of hard chromium coatings, the results suggest that the higher the hardness, the lower is the wear rate under dry conditions (Table 4). Some investigators have observed the wear resistance to improve with increasing hardness while others have found it to deteriorate.[17,19,21-23] The values of the measured COF were high (~0.67-0.69) in comparison with those reported against steel (<0.2). It is well known that COF value is not an intrinsic parameter of material, but the whole tribosystem. It is well known that several mechanisms are involved in the friction generation, which finally resulting in the COF value: plowing of soft surface, adhesion by metalurgical compatibility, presence and interactions of debris and/or oxides.[24] The test configuration and the high mutual solubility between chromium and tungsten (counterbody material) may explain the high friction coefficient measured.[13,25,26]
Figure 5 shows the SEM micrograph of the worn surfaces for HC samples. Wear on HC coatings is dominated by two wear mechanisms: contact fatigue and adhesive wear. Initially, the contact conditions were severe and consequently the wear proccess was characterized by detachment of debris from the coatings in the form of flakes, due to contact fatigue wear. Then, the contact geometry was modified (from non-conforming to conforming) because the wear produced at the beginning. At this point, the contact stress level diminished, and therefore the wear rate mechanism controls the change mechanism to mild adhesive wear. The HC coating with additive have shown a higher wear resistance in the last stage resulting in lower wear rate than those for HC conventional coatings.

ISSN 2179-3956

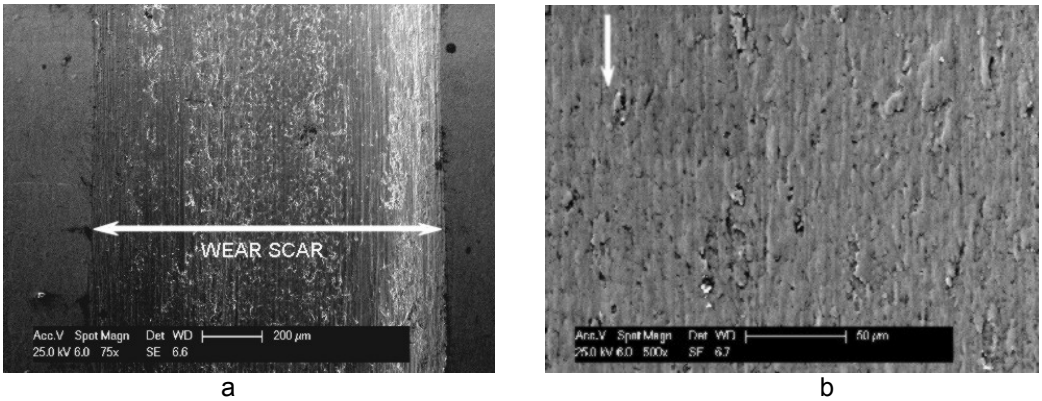

a b

Figure 5. Top-down SEM micrographs of HC with additive sample: (a) general view of wear track at 75X and (b) detail of the center of worn surface at 500X. Arrow point out the sliding direction.

The wear rates of Ni-W and Ni-W-P coatings were much lower than those of HC coatings. This observation can be attributed to the toughness and the microstructure (nanocrystalline structure and crack-free) and also to the enhanced lubricity by P.[27] The best tribological results were obtained on Ni-W DC coatings. It is clear that the surface morphologies with and without wear showed only slight differences on the surface. The damage generates during the tribological process was moderate and is consistent with a type plough-abrasion mechanism, which involves surface damage without loss of material (Figures 6 and 7a). This damage morphology is typically developed in ductile materials. However, this wear mechanism can not take place on HC coatings due to their high level of brittleness.

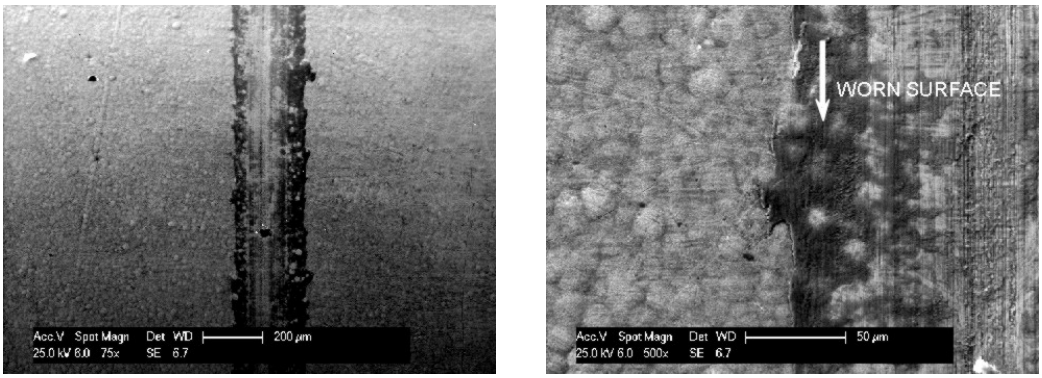

a b

Figure 6. Top-down SEM micrograph of Ni-W DC sample (a) general view of wear track at 75X and (b) detail of the edge of worn surface at 500X.

Ni-P monolayer coatings were more damaged than HC coatings, as it was expected because they are softer than HC coatings (~ 550 against ~ 950 kgf/mm^2, respectively). However, when the same types of coatings were accommodated in a multilayer system, the wear rate decreased nearly two orders of magnitude (Table 4). The lower wear rate was found for the coating composed by 50 layers (Table 4, Figure 8). Also, this coating showed the lowest friction coefficient value (0.35).

ISSN 2179-3956

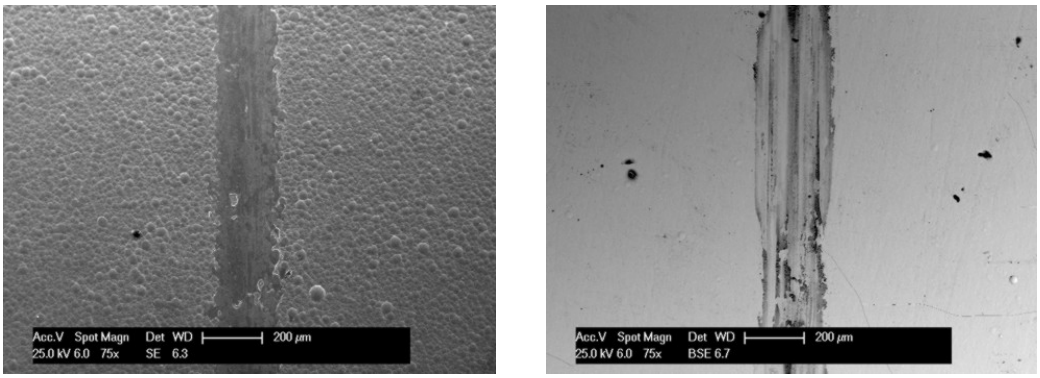

a b

Figure 7. Top-down SEM micrographs about general view at 75X of wear track (a) of Ni-P-W AC sample and (b) Ni-P 50 layers sample.

The morphology of the worn surface of Ni-P multilayered coatings suggest that the wear mechanism was mainly by plough-abrasion although also slight scratch-abrasion was observed (Figure 7b). The lower value of wear rate determined for the 50 layers the coating might be due to good self-lubricating properties[28] and a suitable contact stress distribution.

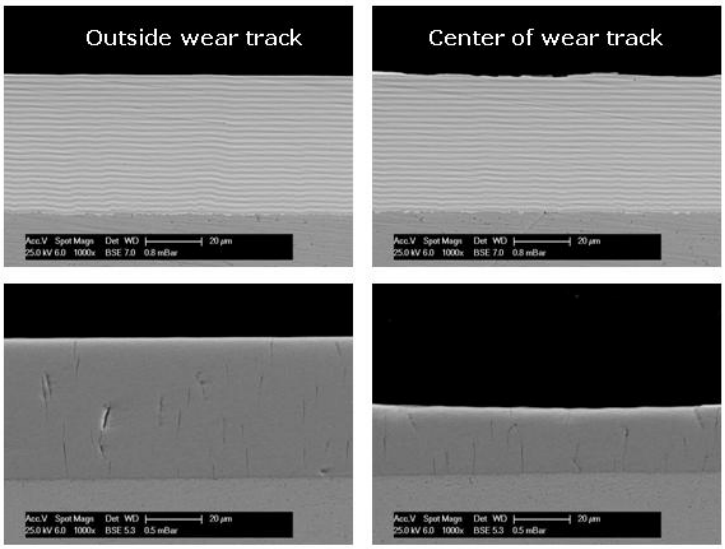

Figure 8. Cross-section SEM micrographs of wear track. On top: Ni-P 50 layers sample at 1000X. On bottom: (b) HC hard chromium sample at 1000X.

4 CONCLUSIONS

Main conclusions on the dry sliding wear behavior can be summarized as follow:

- As-deposited Ni-W, Ni-W-P and Ni-P multilayers coatings exhibit much better sliding wear properties than hard chromium coatings (nearly two order of magnitude higher), even when these possesses higher hardness values, and Ni-P monolayer coatings.

ISSN 2179-3956

- Such differences could be attributable to the wear mechanism. In hard chromium coatings, contact fatigue and mild adhesive wear prevails during the tribological procesess whereas plough-abrasion was observed on Ni-W and Ni-W-P coatings.
- Ni-P multilayered coatings show higher wear resistance than conventional hard chromium and a number of 50 layers appears to be the optimal number.
- Finally, friction coefficients of hard chromium were higher than those of the nickel-based coatings.

REFERENCES

1 SARGENT, G.J. Electrolytic chromium. **Transations American Electrochemical Science**, v. 37, p. 479-497, 1920.
2 FINK, C.G. *US Patent N° 1,581,188,* 1926.
3 HOARE, J.P. On the electrodeposition of chromium. **Journal of Electrochemical Society**, v. 126, n.2, p. 190-199, 1979.
4 LAUSMANN, G.A. Electrolytically deposited hardchrome. **Surface and Coatings Technology**, v. 86-87, p. 814-820, 1996.
5 SHUKER, I., NEWBY, K.R. Why functional trivalent chromium fails and hexavalent chromium is environmentally friendly. **Transactions of the Institute of Metal Finishing,** v. 83, n. 6, p. 272-274, 2005.
6 BROOMAN, E.W. Compliant electrodeposited and electroless nano-structured and nano-composite coatings to replace chromium coatings. **Galvanotechnik**, v. 103, p. 2843-2853, 2005.
7 WESTON, D.P., SHIPWAY, P.H., HARRIS, S.J., CHENG, M.K. Friction and sliding wear behaviour of electrodeposited cobalt and cobalt-tungsten alloy coatings for replacement of electrodeposited chromium. **Wear**, v. 267, p. 934-943, 2009.
8 BERGER, M., WIKLUND, U., ERIKSSON, M., ENGQVIST, H., JACOBSON, S. The multilayer effect in abrasion – optimising the combination of hard and tough phases. **Surface and Coatings Technology**, v. 116-119, p. 1138-1144, 1999.
9 GINES, M.J.L., LOUREIRO, M.J., WILLIAMS, F.J. Effect of phosphorus on the hardness temperature resistance of nanostructure Ni-W electrodeposited coatings. **Plating and Surface Finishing**, v. 96, n. 5, p. 30-35, 2009.
10 JONES, A.R., HAMANN J., LUND, A.C., SCHUH, C.A. Nanocrystalline Ni-W alloy coating for engineering applications, **Plating and Surface Finishing,** v. 97, n. 4, p. 52-60, 2010.
11 YAMASAKI, T., SCHOLOMACHER, P., EHRLICH, K., OGINO, Y., Formation of amorphous electrodeposited Ni-W alloys and their nanocrystallization. **Nanostructured Materials**, v. 10, p. 375-388, 1998.
12 SCHUH, C.A., NIEH,T.G., IWASAKI, H. The effect of solid solution W additions on the mechanical properties of nanocrystalline Ni. **Acta Materialia**, v. 51, p. 431-443, 2003.
13 WANG, L., GAO, Y., XUE, Q., LIU, H. XU, T. A novel electrodeposited Ni-P gradient deposit for replacement of conventional hard chromium. **Surface and Coatings Technology**, v. 200, p. 3719-3726, 2006.
14 KLUG, H.P., ALEXANDER, L.E. **X-ray diffraction procedure**s. 2nd Edition, John Wiley & Sons, 1974.
15 ZANG, Z., ZHOU, F., LAVERNIA, E.J. On the analysis of grain size in bulk nanocrystalline materials via X-ray diffraction. **Metallurgical and Materials Transactions A**, v. 34, p. 1349-1355, 2003.
16 ASSOUL, M., WERY, S., DE PETRIS-WERY, M., GAIGNER, G., MARTI, J. Relationship between tribological properties of hard chromium coatings. **Transactions of the Institute of Metal Finishing**, v. 85, n. 3, p. 135-140, 2007.

ISSN 2179-3956

17 NEWBY, K.R. Why are all functional chromium deposits nor the same? **Transactions of the Metal Fiishers´s Association of India**, v. 5, n. 4, p.237-242, 1996.
18 GAWNE, D.T. Failure of electrodeposited chromium coatings on cast iron substrates. **Thin Solid Fims**, v. 118, p.385-393, 1984.
19 JONES A.R. Hard chromium: microcrak formation and sliding wear. **Transations Institute of Metal Finishing**, v. 70, n.1, p.8-13, 1992.
20 COURNEY, T.H. **Mechanical Behavior of Materials**, Mc Graw-Hill, 1990.
21 BOLELLI, G., CANNILLO, V., LUSVARGHI, L., RICCO, S. Mechanical and tribological properties of electrolytic hard chrome and HVOF-sprayed coatings. **Surface and Coatings Technology**, v. 200, p. 2995-3009, 2006.
22 SOHI, M.H., KASHI, A.A., HADAVI, S.M.M. Comparative tribological study of hard and crack-free electrodeposited chromium coatings. **Journal of Materials Processing Technology**, v. 138, p. 219-222, 2003.
23 ZENG, Z., WANG, L., CHEN, L., ZHANG, J. The correlation between the hardness and tribological behaviour of electroplated chromium coatings sliding against ceramica and steel counterparts. **Surface and Coatings Technology**, v. 201, p. 2282-2288, 2006.
24 ASM METALS HANDBOOK. **Friction, Lubrication and Wear Technology**, Vol 18, ASM International, 1992.
25 HEYDARZADEH SOHI, M., KASHI, A.A., HADAVI, S.M.M. Comparative tribological study of hard and crack-free electrodeposited chromium coatings. **Journal of Materials Processing Technology.** v. 138, p. 219–222, 2003.
26 CHIU, L.H., YANG, C.F., HSIEH, W.C., CHENG, A.S. Effect of contact pressure on wear resistance of AISI H13 tool steels with chromium nitride and hard chromium coatings **Surface and Coatings Technology,** v. 154 p. 282–288, 2002.
27 ASM METALS HANDBOOK. **Surface Engineering**, v. 5, ASM International, 1994.
28 YAN, M., YING, H.G., MA, T.Y., Improved microhardness and wear resistance of the as-deposited electroless Ni-Pcoating, **Surface and Coatings Technology,** v. 202 p. 5909–5913, 2008.